J Seismol (2007) 11:59–72
DOI 10.1007/s10950-006-9037-8

ORIGINAL ARTICLE

The March 2004 Kalamata seismic sequence: a case of efficient seismicity monitoring in the area of Peloponnese, southern Greece, by the Tripoli Seismic Array

M. Pirli · N. Voulgaris · A. Chira · K. Makropoulos

Received: 27 January 2006 / Accepted: 1 September 2006 / Published online: 7 December 2006

Abstract On March 1, 2004, a moderate earthquake occurred in the vicinity of the town of Kalamata, southern Peloponnese, Greece. The Tripoli Seismic Array (TRISAR), located in the centre of Peloponnese, recorded the mainshock as well as the large number of aftershocks that followed. Only a small number of these events were located by regional seismographic networks. Analysis of the Kalamata seismic sequence and evaluation of the results is presented in this article, as an example of the efficiency of TRISAR in seismicity monitoring and location in the area of Peloponnese.

Key words array · sequence · seismicity monitoring · Kalamata · Greece

Introduction

A small-aperture seismic array composed by four 3-component stations was installed on July 16, 2003, in the vicinity of the town of Tripoli, central Peloponnese, Greece, by the Seismological Laboratory of the University of Athens, in order to investigate and assess the contribution of such a system in terms of seismicity monitoring and earthquake location in the area of Greece. Three short-period sensors (CMG-40 T-1 Hz) are located at the peaks of an almost equilateral triangle, whereas a broadband station (CMG-40 T-60 s) is installed in the middle of this deployment. All stations are equipped with 24-bit RefTek 72A-07/G/ND digitizing units storing 30 min records of 125 samples/s sampling rate on 4-Gb RefTek hard disks. Timing is controlled by a GPS unit for each station, synchronizing every 30 min, with precision higher than 1 ms. Array aperture is very small, the side of the triangle being equal to approximately 250 m (Figure 1). Tripoli Seismic Array (TRISAR) elements are situated in the area of the Tripoli airport, which provides a uniform geological setting and no elevation differences throughout the extent of the array (Alexopoulos 1998; Pirli et al. 2004a, 2004b).

Small aperture and number of sensors as well as the lack of a common time base introduce restrictions in array performance. However, the test character of the array permits the extraction of valuable conclusions regarding performance of such a system in the area of Greece. A major interest is expressed in relation to the capabilities of a small-aperture seismic array in Greece, operating as a monitoring system, particularly on a real-time basis. Similar array studies in areas of high seismicity rates have also taken place elsewhere around the Mediterranean, for example, in Italy (Braun et al. 2004).

M. Pirli · N. Voulgaris (✉) · A. Chira · K. Makropoulos
Department of Geophysics–Geothermics,
University of Athens, Panepistimioupolis-Zographou,
157 84 Athens, Greece
e-mail: voulgaris@geol.uoa.gr

Currently, real-time processing is not available for TRISAR; however, a real-time processing simulation was made possible since January 2005, using the Detection Processor (DP), Event Processor (EP) and Regional On-line Array Processing Package (RONAPP) algorithms provided by the Norwegian Seismic Array (NORSAR). Algorithms were adapted to TRISAR configuration by NORSAR staff and appropriately tuned for processing seismicity in Greece in collaboration with the Seismological Laboratory of the University of Athens (Pirli 2005). Final event locations result from manually reviewing automatic system preliminary locations.

Because of its very small aperture, optimum performance in terms of slowness and backazimuth resolution for TRISAR is restricted to an epicentral distance range between 40 and 180 km. High coherence levels for the same epicentral distance range guarantee the validity of slowness vector estimations (Figure 2). Automatic backazimuth estimation standard deviation within 80 km distance from the array has been calculated in the order of 7° and increases with epicentral distance (Pirlis 2006). For this distance range, TRISAR achieves a magnitude of completeness in the order of 2.0 on the local magnitude scale, whereas independently of epicentral distance TRISAR magnitude of completeness is in the order of 3.3. Regions included within the optimum distance range are the broader area of the Peloponnese, the broader Gulf of Corinth and Attica region, as well as Evia Island. A vast number of earthquakes from these regions (more than 10,000 events during the first 9 months of operation) have been detected and catalogued, especially from the area of the Peloponnese (Pirli 2005). More than 3500 of these events have been located, while location of the rest of the detected events is in progress, and results will be included in a future research.

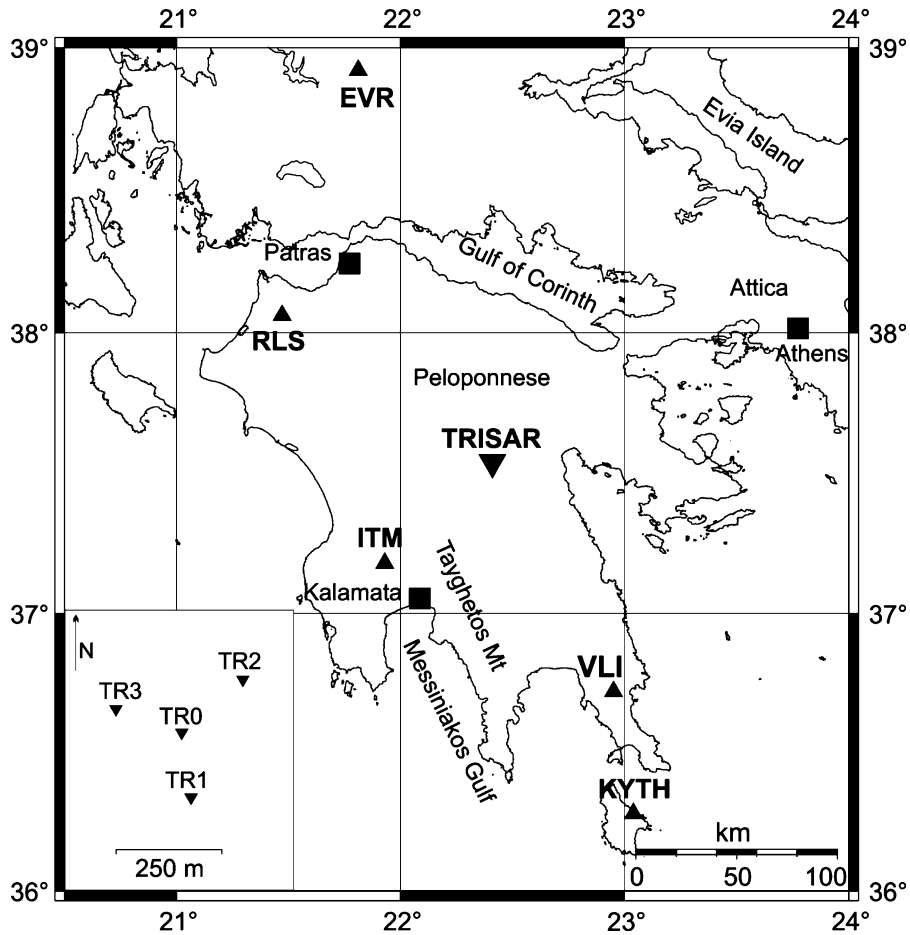

Figure 1 Map of the broader Peloponnese area. Location and geometry of the Tripoli Seismic Array (TRISAR) and locations of NOA stations providing phase data for the Kalamata aftershocks location.

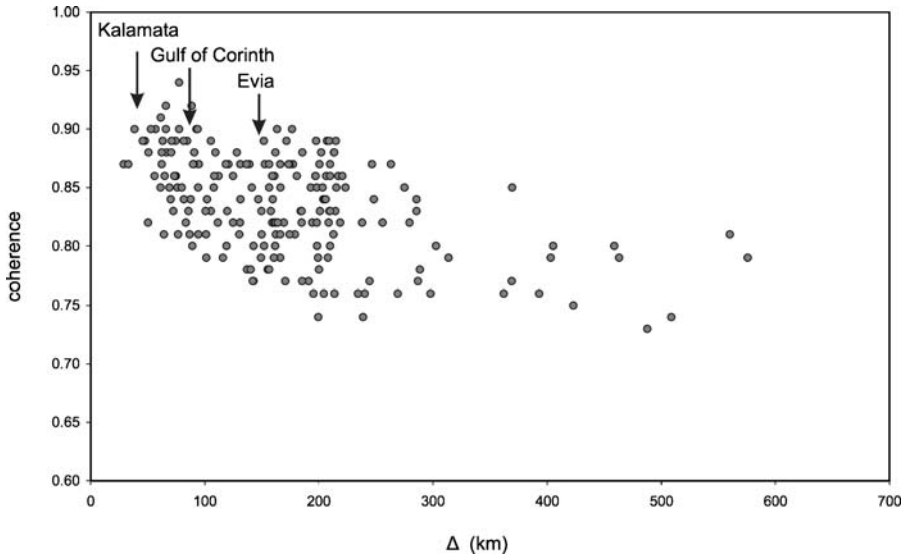

Figure 2 Spatial coherence distribution versus epicentral distance for a dataset of 200 seismic events from the area of Greece (Pirli 2005) recorded by TRISAR.

However, the most striking example of efficient TRISAR performance, in terms of monitoring within the array optimal performance distance range, when compared to that of national and regional networks, is the Kalamata seismic sequence, which took place on March 2004. The mainshock (1 March 2004, 00:35:58.36 GMT) was a moderate earthquake (Mw= 5.3) that occurred NE of the town of Kalamata. The National Seismographic Network of the Geodynamics Institute of the National Observatory of Athens (NOA) located a total of 10 events within a time interval of 40 days. For the same period, TRISAR, which is located at an epicentral distance of approximately 40 km from the aftershock area, analysed and located more than 100 aftershocks. The seismic sequence was also recorded by the seismographic network operated by the University of Patras, with the total number of located events being still much lower compared to that provided by TRISAR. These facts suggest the great significance of TRISAR as a means to monitor seismic activity in the Peloponnese.

Data processing and analysis

Since January 2005, TRISAR data have been organized into CSS3.0 flatfiles, a database schema linking waveform data to tables containing several information, such as recording stations' characteristics, etc. (Anderson et al. 1990; Carr 2002), and have been undergoing a real-time detection and processing simulation with the DP, EP and RONAPP software developed at NORSAR (Mykkeltveit and Bungum 1984; Fyen 1987, 1989). Automatic algorithm results are being reviewed by an analyst. Before the NORSAR software became available, the procedure being followed consisted of an analyst compiling a recorded events list and the manual processing of the identified earthquakes. In the case of the Kalamata sequence, identification of events belonging to the same activity was an easy task for the analyst, due to the high level of waveform similarity between the vast majority of the aftershocks (Figure 3) and the characteristic S–P arrival time difference observed (6.2±0.4 s).

The approach presented in this report is the automatic analysis preceding the manual review, in order to draw conclusions regarding the efficiency of simulated real-time analysis for a dataset of high coherence levels. An STA/LTA threshold detector (Schweitzer et al. 2002) specially parameterized for TRISAR data (Pirli 2005) is used to detect phases belonging to seismic events. The slowness vector is calculated for each detected phase, using broadband *f–k* analysis (Kværna and Ringdal 1986) and then individual phases are grouped into events, which are located by applying the TTAZLOC algorithm (Bratt and Bache 1988). Automatic algorithms' performance is restricted by TRISAR low backazimuth and slowness resolution, an effect of array geometry,

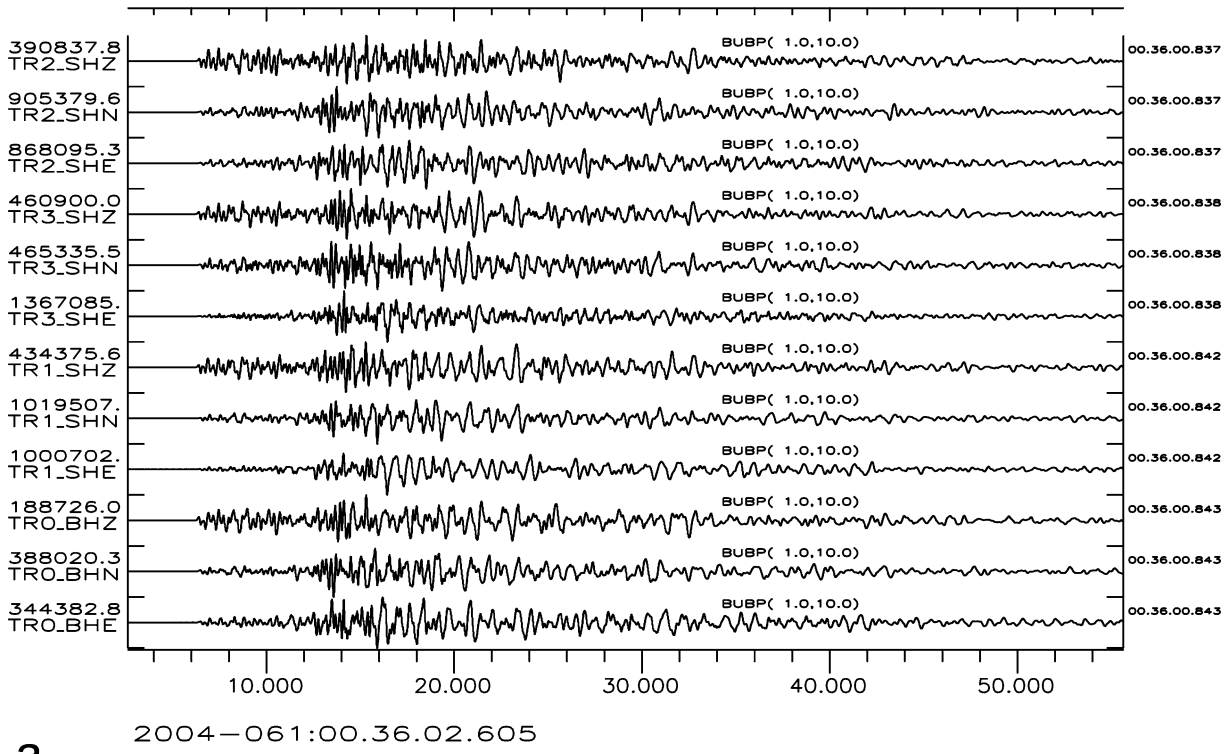
390837.8
TR2_SHZ
905379.6
TR2_SHN
868095.3
TR2_SHE
460900.0
TR3_SHZ
465335.5
TR3_SHN
1367085.
TR3_SHE
434375.6
TR1_SHZ
1019507.
TR1_SHN
1000702.
TR1_SHE
188726.0
TRO_BHZ
388020.3
TRO_BHN
344382.8
TRO_BHE
BUBP(1.0,10.0)
00.36.00.837
00.36.00.837
00.36.00.837
00.36.00.838
00.36.00.838
00.36.00.838
00.36.00.842
00.36.00.842
00.36.00.842
00.36.00.843
00.36.00.843
00.36.00.843
10.000
20.000
30.000
40.000
50.000
2004—061:00.36.02.605

a

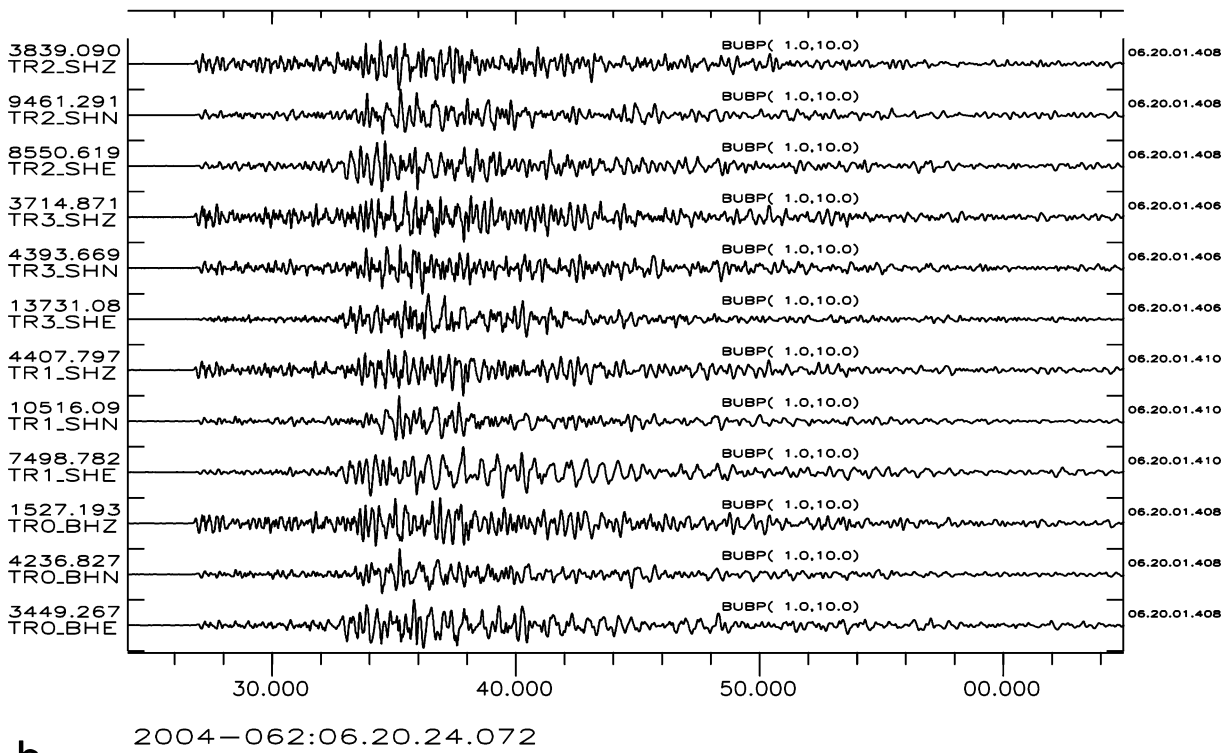
3839.090
TR2_SHZ
9461.291
TR2_SHN
8550.619
TR2_SHE
3714.871
TR3_SHZ
4393.669
TR3_SHN
13731.08
TR3_SHE
4407.797
TR1_SHZ
10516.09
TR1_SHN
7498.782
TR1_SHE
1527.193
TRO_BHZ
4236.827
TRO_BHN
3449.267
TRO_BHE
BUBP(1.0,10.0)
06.20.01.408
06.20.01.408
06.20.01.408
06.20.01.406
06.20.01.406
06.20.01.406
06.20.01.410
06.20.01.410
06.20.01.410
06.20.01.408
06.20.01.408
06.20.01.408
30.000
40.000
50.000
00.000
2004—062:06.20.24.072

b

◀ **Figure 3** (a) The 1 March 2004 Kalamata mainshock as recorded by the three components of the four elements of TRISAR. (b) An aftershock of the 2004 Kalamata sequence, as recorded by TRISAR.

resulting in large uncertainties in backazimuth estimation and frequent phase misidentifications, especially for earthquakes located at epicentral distances larger than 200 km (Pirli 2005).

Automatic system results are reviewed by an analyst in order to check for errors in phase detection and identification, as well as onset-time determination, and the final epicentre solution is calculated using the HYPOSAT algorithm (Schweitzer 2001a). For analysis of the Kalamata sequence events, a local model compiled by Lyon-Caen et al. (1988) using the Kalamata 1986 seismic sequence data (Table 1) was employed to describe the upper crust. Lower crust and upper mantle were simulated using the regional MENA1.0 velocity model (Sweeney and Walter 1998) for the area of Greece and Asia Minor, modified slightly with the addition of one deeper layer simulating the upper mantle (Pirli 2005), according to information derived from the literature (e.g., Ligdas et al. 1990; Spakman 1991; Papazachos and Nolet 1997). Mean error values in epicentre coordinate and origin time determination are in the order of 4.5 km in the N–S direction, 7.8 km in the E–W direction and 0.6 s, respectively.

Automatic detection and analysis procedure produced poor results, detecting both a P and S phase for approximately only 50% of the recorded aftershocks, in respect to the volume listed in the manually compiled catalogues. For the rest of the events, only a single phase has been detected automatically, thus prohibiting automatic event location. Such a result was expected, since in general power detectors may perform poorly when processing aftershock sequences with frequently overlapping events. This problem is intensified by the low slowness and backazimuth resolution of the array that causes frequent phase misidentifications and wrong phase grouping into events that can be located. Despite insufficient automatic algorithm performance and the low gain achieved by beamforming ($\sqrt{4}$) using a four-element array (e.g., Schweitzer et al. 2002), two aftershocks were detected exclusively by the automatic detector. These were exceedingly low signal/noise ratio (SNR) value cases, not discernible under the bandpass filter applied during routine processing and therefore missed by the analyst. Automatic detection lists, as usually done with TRISAR data processing, have been reviewed by an analyst, who eliminated false alarms and catalogued single phases for manual processing and location of corresponding events. Thus, it is ascertained that the whole seismicity volume has been analysed and located.

Table 1 Velocity model used for locating the Kalamata sequence

Depth (km)	V_p (km/s)	V_s (km/s)
0.0	5.00	2.80
2.0	5.40	3.05
5.0	6.00	3.40
13.5	6.60	3.70
24.0	7.20	4.00
34.0	7.90	4.46
100.0	8.00	4.49

Epicentres calculated by the automatic algorithm are depicted in Figure 4. The obtained image corresponds to significantly more diffused seismicity than expected in the case of a seismic sequence, the aftershocks being spread over a large area. No conclusions regarding the characteristics of the analysed activity may be drawn from the resulting distribution, as no actual concentration of epicentres seems to appear. It is clear, therefore, that the obtained image is an artefact due mainly to low backazimuth resolution of the Tripoli Array, which affects the quality of performance of the automatic algorithms. However, provided results may prove useful for a very preliminary image of the activity in the area under investigation in terms of monitoring, especially under the assumption of real-time data processing.

Local magnitude M_l was also calculated by the automatic algorithm, using a Wood–Anderson simulation trace, produced from the seismic records, as well as the epicentral distance calculated by the TTAZLOC algorithm (Pirli 2005). Because automatic solutions are frequently characterised by large deviations in epicentral distance determination and phase misidentifications, a re-estimation of the local magnitude took place, using the empirical formula suggested by Kiratzi (1984) for the area of Greece:

$$M_l = \log\ a + 2.32\ \log\ R - 1.1 \qquad (1)$$

where a the amplitude of true ground displacement (μm) and R is the hypocentral distance (km). The

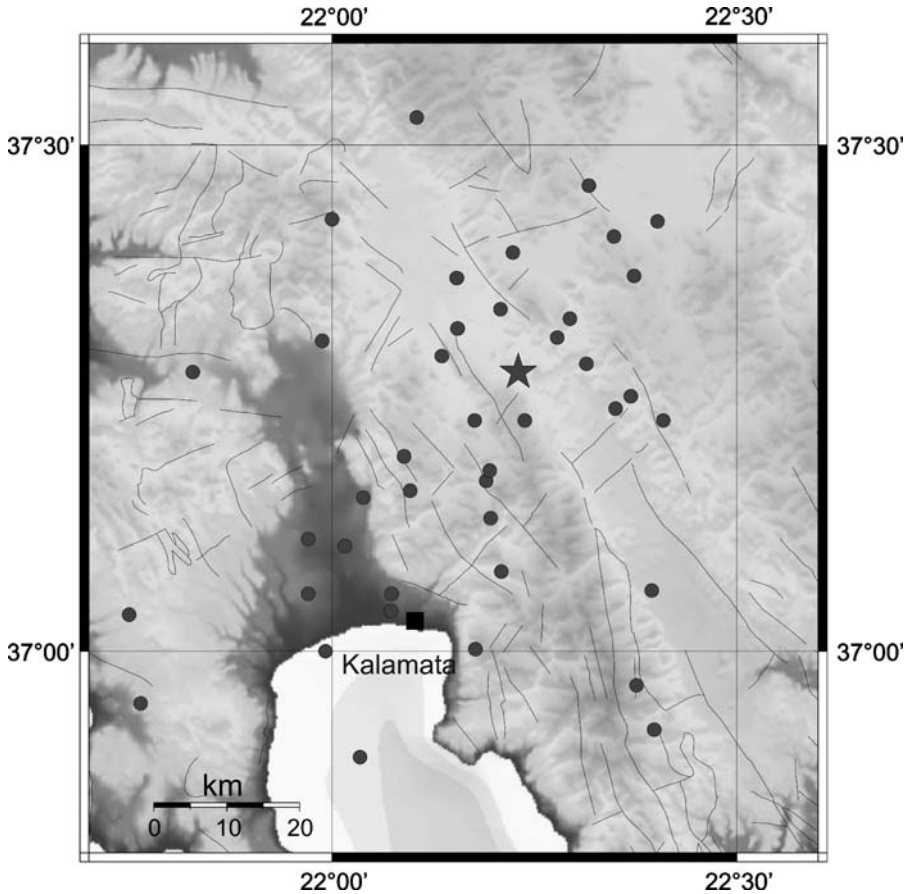

Figure 4 Spatial distribution of the Kalamata sequence events, as located by the automatic algorithm used for TRISAR data processing. Location of the mainshock is marked by a star. Major faults in the area are also depicted according to IGME (1989).

epicentral distance is used instead, because TRISAR single location results lack information concerning focal depth. This is expected to result in a deviation from magnitude values reported by other sources; nonetheless, the obtained reduction is expected to be systematic and not seriously affect calculations of Gutenberg–Richter law, presented later in this report.

The data used in this contribution cover a time interval of 40 days from the occurrence of the mainshock. Within this period, TRISAR recorded and located a total of 122 events from the same sequence. The aftershocks are distributed within an area situated at the northern part of Tayghetos Mountain, northeast of the town of Kalamata. Their spatial distribution (Figure 5) is extending almost parallel to the E–W direction, being characterised by intense scatter. A significant cluster of aftershocks is located directly to the south of the epicentre of the mainshock. The rest of the aftershocks are distributed both to the west and the east of this concentration, while a larger number of epicentres is observed in the western part. Up to a certain degree, such a distribution could be attributed to restricted TRISAR resolution in backazimuth determination; however, it should be noted that for epicentral distances of less than 80 km, the array achieves satisfactory accuracy with respect to event location (Pirli 2005).

Comparison of the reviewed results to the epicentre distribution acquired by the automatic algorithm reveals that no systematic mislocation can be observed for TTAZLOC epicentres. In fact, some cases are located further to the north, compared to the 'true' locations, while others appear to have moved more towards the South. This can only reflect the diversity of problems met by the automatic processing system. Moreover, it implicates no systematic backazimuth standard deviation that could be interpreted as a backazimuth anomaly that could be corrected for.

This image acquired by TRISAR data deviates significantly from that obtained by NOA locations (http://www.gein.noa.gr). According to NOA, only nine events apart from the mainshock are distributed

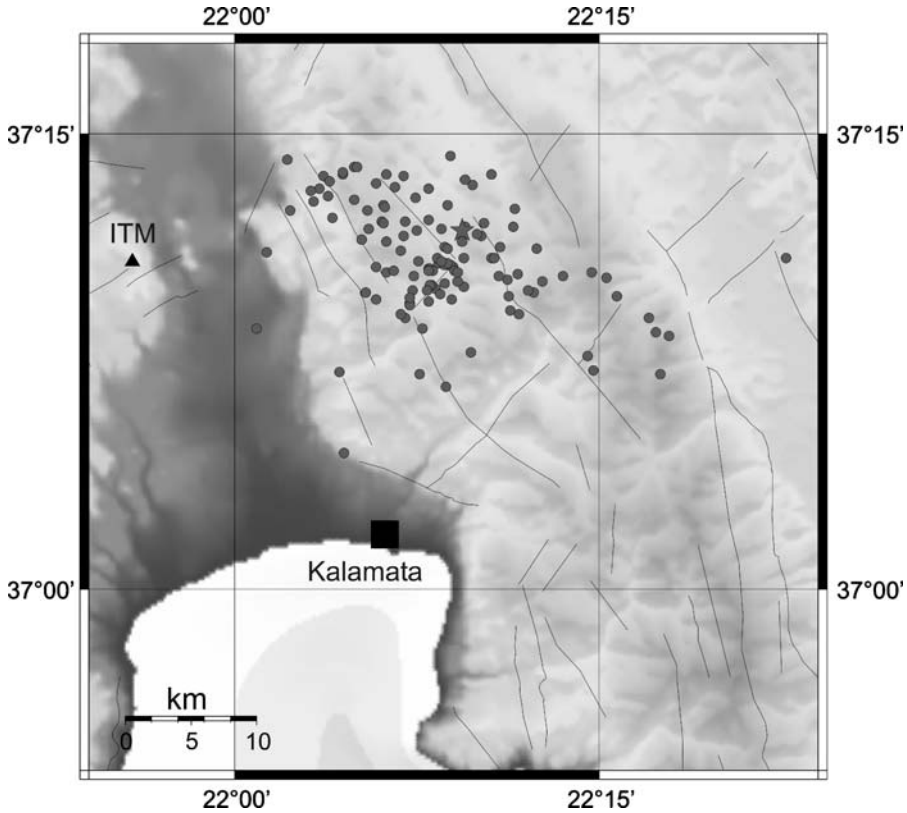

Figure 5 The Kalamata mainshock (star) and aftershock sequence (circles), as located by an analyst, from TRISAR records. Major faults in the area are also depicted according to IGME (1989).

in the N–S direction, covering an area which extents from northern Tayghetos Mountain to Messiniakos Gulf (Figure 6a). This would imply an activation of approximately 30 km, inconsistent with the moderate magnitude of the mainshock and the relatively small magnitudes observed throughout the aftershock sequence. Furthermore, the very small number of aftershocks recorded and located by NOA does not reflect the true characteristics of the sequence under investigation. It should be made clear though that the significant difference in the number of analysed events by the two networks strongly suggests that it is difficult to substantiate a differentiation regarding the overall character of the seismic sequence, as reported by NOA and TRISAR.

To further investigate this observed deviation between the two solutions, location results from the seismographic network of the University of Patras (http://www.seismo.geology.upatras.gr) were also taken into account. As noted earlier, the number of events located by the University of Patras is also very small compared to the volume located by TRISAR. In this case, the distribution of aftershocks follows the one resulting from TRISAR data (Figure 6b). The main difference between the two distributions is the fact that in the case of Patras data, aftershocks appear to concentrate in the eastern part of the area covered by TRISAR located events and slightly to the south. The problem of uneven number of aftershocks located between the two networks remains, so only the general trend depicted may be evaluated. However, the image obtained by Patras data appears to be in agreement with the E–W distribution resulting via TRISAR data.

Regarding location accuracy, 95% confidence level error ellipsoids have been calculated (Schweitzer 2001a). Determination was not possible only in nine cases, due to the large standard deviation in backazimuth estimation that excluded these values from the inversion process. Backazimuth standard deviation is the main contributor to the resulting error ellipsoids, as slowness is rarely used for epicentre determination in such local distances and onset-time residuals are in general small, due to the good quality of TRISAR recordings for the particular sequence and the significant similarity of the aftershock waveforms. Length of major and minor axis (in km) is plotted

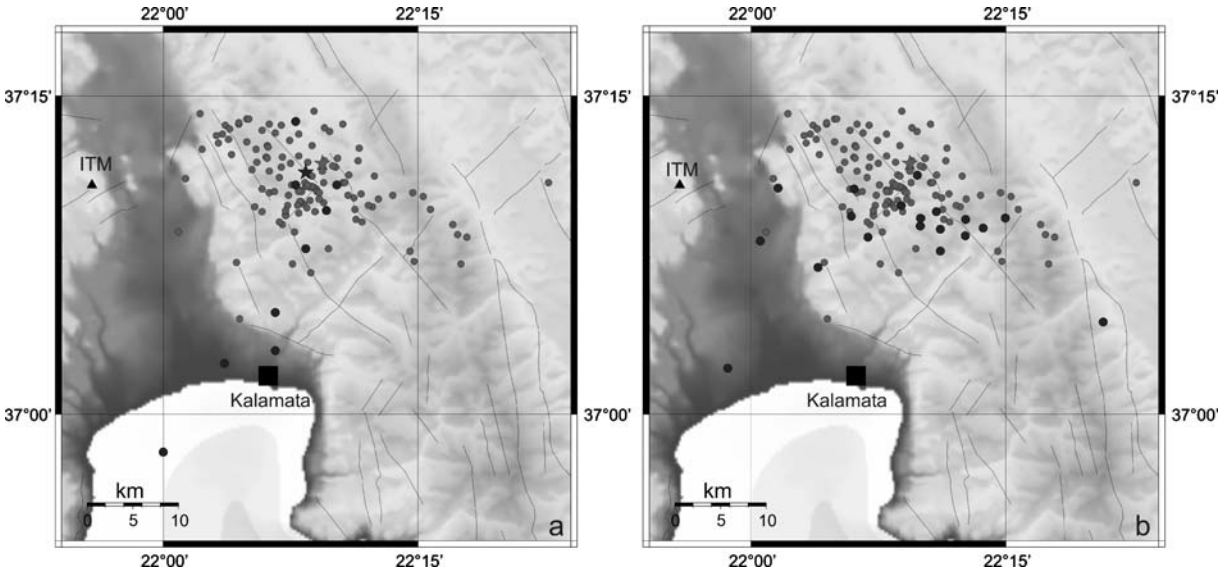

Figure 6 (a) TRISAR locations (light colour) and NOA locations (dark colour) for the Kalamata sequence. (b) TRISAR locations (light colour) and University of Patras locations (dark colour) for the Kalamata sequence. In both (a) and (b), location of the mainshock is marked by a star. Major faults in the area are also depicted according to IGME (1989).

against the number of events in the histogram in Figure 7. It is evident that for the vast majority of the events belonging to the Kalamata sequence, both axes are less than 10 km long. An elongation of the error ellipsoid observed for the 12 events with major axis larger than 20 km reflects the restricted backazimuth resolution achieved by TRISAR. Taking into consideration all the restrictions imposed on array performance by its design, the achieved accuracy can be characterised as quite satisfactory in terms of seismicity monitoring, although it is clearly insufficient for seismotectonic interpretation of the phenomenon. The rose diagram of Figure 7 depicts the distribution of the number of error ellipsoids versus azimuth. Most of the calculated ellipsoids appear to be elongated parallel to a NW–SE direction of an approximately 135° trend, as well as a 115° trend. This observation also suggests that the observed spatial distribution of the aftershocks may be affected by large backazimuth standard deviation in the slowness vector calculations.

Regarding the magnitude of the aftershocks, calculated values are quite small. This is consistent

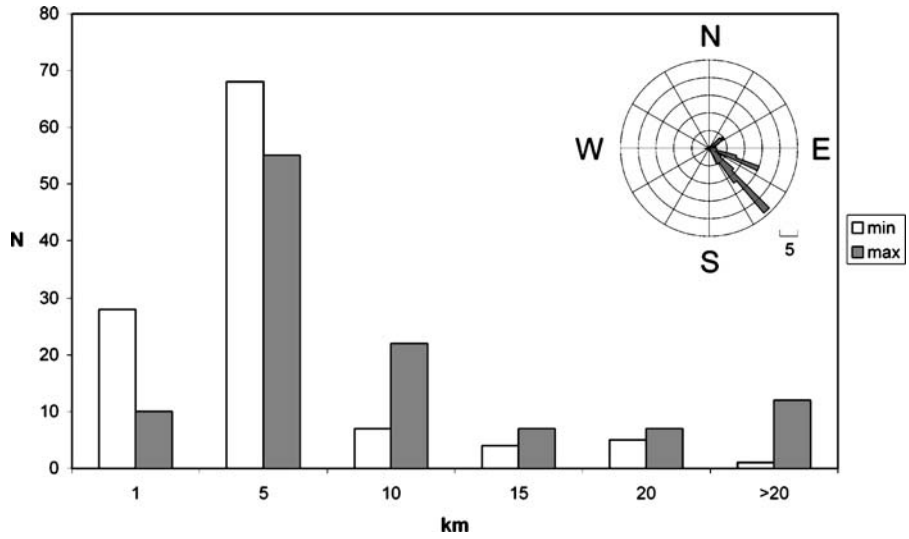

Figure 7 Histogram of the distribution of error-ellipsoid axes' dimensions per number of events and rose diagram for ellipsoid azimuth distribution.

with the small values also reported by NOA at the time of occurrence, which – combined with the small number of aftershocks located by that source – had resulted in significant concern regarding the evolution of the seismic sequence. The Gutenber–Richter law for this sequence was determined by using the reviewed local magnitude values from TRISAR data, in order to evaluate the characteristics of the Kalamata aftershock sequence. The diagram depicting the relation between local magnitude M_l and log N is presented in Figure 8. The resulting relation is described by:

$$\log N = -1.26M_l + 4.67 \quad (2)$$

Both of a and b values are characteristic of an aftershock sequence in Greece (Hatzidimitriou et al. 1985), indicating that the Kalamata activity was in fact a typical case of seismic sequence. As made clear in the diagram in Figure 8, the magnitude of completeness for this particular sequence, as recorded by TRISAR, is 2.1 on the local magnitude scale. Low aftershock magnitude values are consistent with the moderate magnitude of the main shock, and probably the fact that the broader area had been discharged by the activity related to the 1986 Kalamata seismic sequence (Lyon-Caen et al. 1988), located directly to the south of the 2004 activity (Figure 9).

To investigate any potential improvement of aftershock locations, seismic onset observations for the Kalamata sequence have been requested and obtained from NOA. These observations, however, concern the same dataset for which locations have been published on the institute's website. A further search was made in the ISC web resources (http://www.isc.ac.uk/Bull) and phases from NOA stations were recovered for only two additional events. In this context, no actual conclusions may be drawn regarding the possibility of enhancing locations, due to the very small amount of available data and also to the contributing station distribution, as previously depicted in Figure 1. A purely indicative image can be obtained and, therefore, joint location results by using both TRISAR and NOA data are presented.

Table 2 provides the obtained location results, as well as information on errors in the location process and error-ellipsoid dimensions. Each event is listed by a reference number (Ref), its origin time, epicentre coordinates and depth value, as well as error in N–S and E–W direction in degrees, timing error (DTo) in seconds, number of defining records (Def), RMS and error-ellipsoid axes dimension in km, ellipsoid azimuth and area coverage (km^2). All events have been relocated using the regional MENA1.0 velocity model (Sweeney and Walter 1998), as recording stations are situated at large distances from the epicentral area. Lack of information concerning the actual uncertainties in NOA phase picks was compensated for by the introduction of fixed values according to reported onset quality provided in the International Seismological Centre (ISC) phase catalogues (Rodi 2006; Schweitzer 2006) and also taking into consideration the proximity of recording stations. ISC calculated focal depth for the mainshock resulted in 14 and

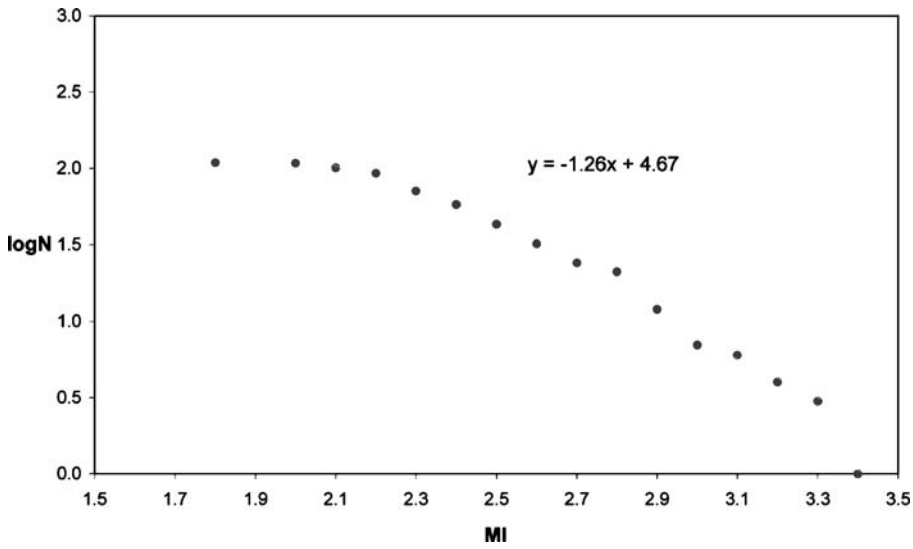

Figure 8 Gutenberg–Richter law for the March 2004 Kalamata aftershock sequence.

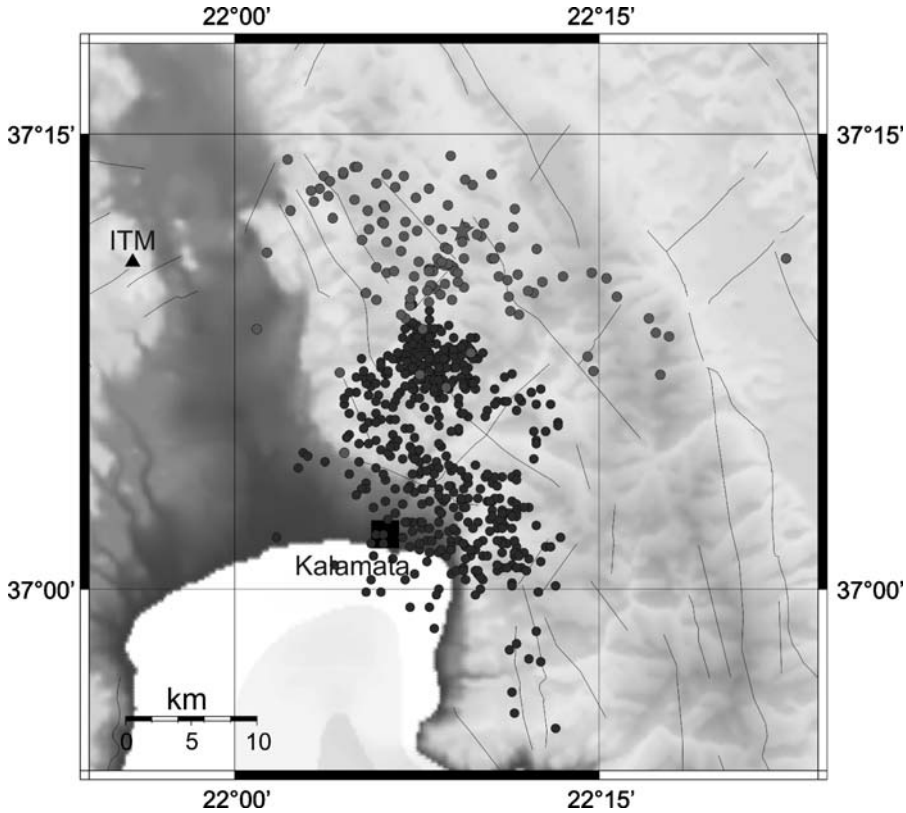

Figure 9 Epicentre distribution of the March 2004 Kalamata sequence (light colour) by TRISAR data and epicentre distribution of the September 1986 sequence (dark colour), as calculated by Lyon-Caen et al. 1988. Major faults in the area are also depicted according to IGME (1989).

17 km with the use of pP phases (International Seismological Centre 2001). Since no adequate resolution can be achieved with the available data, depth was fixed at a value of 15 km for the mainshock, as well as the relocated aftershocks. It is evident that in general errors are characterised by very low values and major axes of error-ellipsoids do not exceed the length of 5 km in most cases. Increases in ellipsoid dimensions compared to single array locations, as in the case of the mainshock, are expected, since ellipsoid dimensions increase with the usage of large absolute uncertainty values.

Spatial distribution of the jointly located events and the corresponding 95% confidence level error-ellipsoids are presented in Figure 10. Resulting epicentres appear to be more consistent to single TRISAR locations than reported NOA calculations (http://www.gein.noa.gr). Table 3 provides the overall deviation between the different solutions in km, as well as the angle from the joint to the individual solution (azimuth), both with respect to NOA and TRISAR locations. Whenever a location had not been reported by NOA, the result appearing in the ISC On-line Bulletin is used. This provides information regarding the direction in which the epicentre of each event has moved after joint relocation. No systematic pattern can be observed regarding direction; however, from the table it also becomes clear that joint locations are closer to single array results than individual NOA locations. This can be expected, taking into consideration the distribution of recording stations. Most of the aftershocks located by NOA are recorded by stations ITM, VLI, RLS, KYTH and EVR (Figure 1), a distribution which is characterised by a large gap in azimuthal coverage in the NE of the Kalamata activity area. This gap is covered by TRISAR, thus moving the epicentres closer to the main volume of the aftershock sequence.

Conclusions

The seismic sequence that occurred close to the town of Kalamata, southern Peloponnese, in March 2004 was recorded and located by TRISAR. This was the

Table 2 Joint location results and corresponding errors in event location

Ref.	Origin time	Lat.	Long.	Depth (km)	D_{lat}	D_{long}	DTo	Def	RMS	Major	Minor	Azimuth	Area
1	2004/03/01 00:35:59.729	37.209	22.148	15	0.0396	0.0528	0.540	41	1.357	3.36	2.27	73.0	24.00
2	2004/03/01 03:44:42.186	37.171	22.122	15	0.0195	0.0188	0.306	10	0.331	1.72	1.58	112.3	8.53
3	2004/03/01 16:27:51.792	37.225	22.090	15	0.0132	0.0166	0.166	9	0.176	1.58	1.30	111.0	6.44
4	2004/03/02 06:20:19.306	37.169	22.168	15	0.0849	0.1152	1.183	10	2.084	7.98	7.10	117.6	272.14
5	2004/03/03 06:06:25.055	37.122	22.129	15	0.0341	0.0387	0.628	15	0.686	3.38	2.94	113.4	31.20
6	2004/03/04 20:56:46.888	37.175	22.118	15	0.0355	0.0376	0.438	8	0.357	4.39	2.11	160.1	29.06
7	2004/03/15 23:42:03.085	37.208	22.108	15	0.0197	0.0217	0.276	11	0.686	1.83	1.75	107.4	10.06
8	2004/03/19 04:19:21.427	37.165	22.118	15	0.0393	0.0434	0.456	9	0.431	5.12	2.17	159.3	34.99
9	2004/03/19 18:01:37.030	37.204	22.046	15	0.0240	0.0270	0.545	10	0.826	4.14	2.00	68.2	26.04
10	2004/03/19 20:23:16.506	37.155	22.080	15	0.0339	0.0455	0.490	10	0.527	3.50	3.17	101.0	34.80
11	2004/03/29 11:59:23.414	37.205	22.085	15	0.0237	0.0263	0.222	9	0.207	3.08	1.19	155.6	11.56
12	2004/04/08 08:38:34.700	37.208	22.080	15	0.0274	0.0361	0.325	12	0.848	3.41	1.87	144.4	20.00
13	2004/04/12 13:40:55.922	37.206	22.082	15	0.0417	0.0466	0.346	8	0.363	5.71	1.90	155.7	34.04

only network that achieved a complete recording of the aftershock sequence down to a magnitude of 2.1 on the local magnitude scale, providing the possibility of analysing its characteristics. Hence, it became evident that this activity was a typical aftershock sequence, located immediately to the north of the area activated during the 1986 Kalamata earthquake and its aftershock sequence.

This is an example of the very efficient monitoring capabilities of TRISAR within the broader Peloponnese region. Although the detector employed for TRISAR data processing faces problems when handling overlapping aftershock events, analyst review provides a more accurate analysis of the activity in the investigated area. This fact can be attributed to the relatively small distance of TRISAR from the aftershock area (a mean epicentral distance of 40 km), which places the analysed sequence within the optimal array performance distance range, in terms of slowness resolution, waveform coherence and event location accuracy.

Precision of epicentre location is affected by imposed restrictions in TRISAR design requiring analyst revision. Indeed, from the dimensions of the calculated 95% confidence level error ellipsoids, it is evident that for the largest percentage of Kalamata aftershocks, analyst location is satisfactorily precise, although certainly inadequate for any seismotectonic interpretation. It can be expected that the achieved accuracy in epicentre determination can be further improved by adding to the solutions only two or three local stations, as observed in the case of recorded seismicity in the Gulf of Corinth (Pirli et al. 2004a, 2004b; Pirli 2005), where a significant reduction of error ellipsoid dimensions was observed for joint TRISAR and single stations location results. Such a possibility may also provide information on the focal depth of the events, which cannot be calculated by single-array location.

Spatial distribution of NOA stations providing phases for the Kalamata activity and the very small amount of available data did not help in extracting

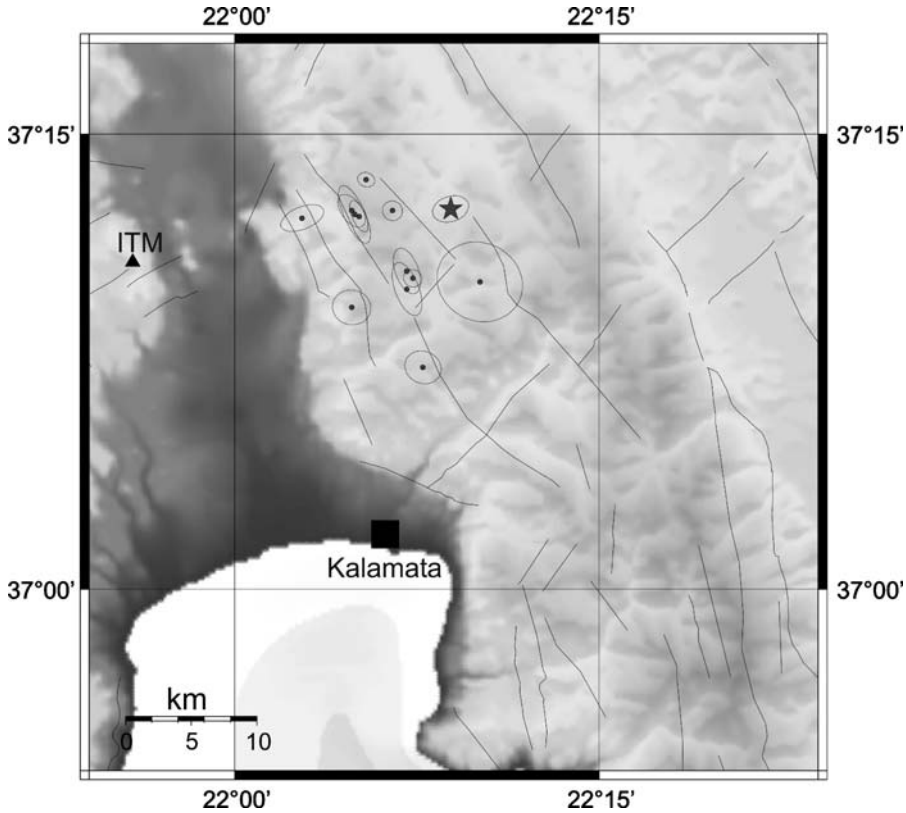

Figure 10 Epicentre distribution and corresponding error-ellipsoids for the events located jointly, using both TRISAR and NOA phase data. Major faults in the area are also depicted according to IGME (1989).

solid conclusions on the above-mentioned assumption. A much larger dataset might have proven more useful in this direction, even though with the existing station configuration TRISAR contributes in terms of event location as an additional single station. However, a detailed account of TRISAR interaction with regional networks and 3-C stations and the contribution of such a system to earthquake location in the region is beyond the scope of this paper and will be addressed in a future research.

Improving array performance and, in particular, automatic algorithm capabilities in monitoring and

Table 3 Deviations between joint and individual solutions according to the event reference number (Ref) of Table 2

Ref	NOA – Joint		TRISAR – Joint	
	Distance (km)	Azimuth (°)	Distance (km)	Azimuth (°)
1	2.23	18.6	1.51	331.9
2	24.81	25.9	1.83	241.0
3	3.59	261.1	5.21	287.4
4	1.23	35.4	6.75	17.6
5	4.96	19.9	7.09	42.6
6	13.89	2.9	6.75	271.9
7	6.32	299.5	2.23	198.6
8	1.98	212.6	5.50	351.6
9	11.71	314.6	3.00	45.3
10	12.89	7.9	4.06	10.1
11	31.78	31.1	1.60	86.0
12	6.95	296.6	5.96	307.9
13	24.60	12.9	0.83	254.5

locating aftershock sequences calls for adopting different approaches than an STA/LTA threshold detector, such as techniques based on waveform cross-correlation (e.g., Harris 1991; Shearer 1997; Schaff and Richards 2004). Waveform similarity in the case of the sequence analysed in this paper is indeed striking, suggesting that a correlation-based detector (Gibbons and Ringdal 2006) may perform exceedingly well.

Although, in the case of the Kalamata sequence, there is no evidence of an existing backazimuth anomaly, overall array performance can be optimised by array calibration with the calculation and introduction of appropriate slowness, backazimuth and/or travel-time station corrections (Schweitzer 2001b).

TRISAR performance in the case of the aftershock sequence presented here suggests that real-time data acquisition and processing for a small-aperture array of this type, can prove to be an important tool in monitoring seismicity in nearby areas of interest in case of a seismic crisis.

Acknowledgments The DP, EP and RONAPP software was kindly provided by NORSAR within the framework of the ARI program (HPRI-CT-2002-00189) funded by the European Commission. The authors would like to thank Johannes Schweitzer for adapting NORSAR algorithms to TRISAR configuration, as well as for discussing the contents of this publication. Two anonymous reviewers have provided useful comments and suggestions for improving this manuscript. NOA phase data were made available within the framework of the action 'IRAKLEITOS, Fellowships for Research, ENVIRONMENT', co-funded within Op. Education by the ESF (European Social Fund) and National Resources. Research was funded within the framework of the program 'Kapodistrias' of the National and Kapodistrian University of Athens. Maps included in this paper were created using the GMT software package (Wessel and Smith 1991, 1998).

References

Alexopoulos J (1998) A contribution to the investigation of the hydrogeological regime of the Tripoli plateau, using geophysical methods. PhD thesis, University of Athens, Athens, p 275 (in Greek)

Anderson J, Farrell WE, Garcia K, Given J, Swanger H (1990) Center for Seismic Studies Version 3 Database Schema Reference Manual. Technical Report C90-01, SAIC-90/1235. Science Applications International Corporation, San Diego, California, p 64

Bratt SR, Bache TC (1988) Locating events with a sparse network of regional arrays. Bull Seismol Soc Am 78:780–798

Braun T, Schweitzer J, Azzara RM, Piccinini D, Cocco M, Boschi E (2004) Results from the temporary installation of a small aperture seismic array in the Central Apennines and its merits for local event detection and location capabilities. Ann Geophys 47:1557–1568

Carr D (2002) National Nuclear Security Administration Knowledge Base Core Table Schema Document, SAND2002-3055, Sandia National Laboratories, p 70

Fyen J (1987) Improvements and modifications. NORSAR Sci. Report No. 2-86/87

Fyen J (1989) Event processor program package. NORSAR Sci. Report No. 2-88/89

Gibbons SJ, Ringdal F (2006) The detection of low magnitude seismic events using array-based waveform correlation. Geophys J Int 165:149–166

Harris DB (1991) A waveform correlation method for identifying quarry explosions. Bull Seismol Soc Am 81:2395–2418

Hatzidimitriou PM, Papadimitriou EE, Mountrakis DM, Papazachos BC (1985) The seismic parameter *b* of the frequency–magnitude relation and its association with the geological zones in the area of Greece. Tectonophysics 120:141–151

IGME (1989) Seismotectonic Map of Greece, scale 1:500000. Institute of Geology and Mineral Exploration (IGME), Athens 1989

International Seismological Centre (2001) On-line Bulletin, http://www.isc.ac.uk/Bull, International Seismological Centre, Thatcham, United Kingdom

Kiratzi AA (1984) Magnitude scales for the earthquakes of the broader area of Greece. PhD thesis, University of Thessaloniki, Thessaloniki, p 171 (in Greek)

Kværna T, Ringdal F (1986) Stability of various *f–k* estimation techniques. NORSAR Semiannual Tech Summ, 1-86/87, 29–40

Ligdas CN, Main IG, Adams RD (1990) 3-D structure of the lithosphere in the Aegean region. Geophys J Int 102:219–229

Lyon-Caen H, Armijo R, Drakopoulos J, Baskoutas J, Delibassis N, Gaulon R, Kouskouna V, Latoussakis J, Makropoulos K, Papadimitriou P, Papanastassiou D, Pedotti G (1988) The 1986 Kalamata (South Peloponnesus) earthquake: Detailed study of a normal fault, evidences for east–west extension in the Hellenic Arc. J Geophys Res 93:14967–15000

Mykkeltveit S, Bungum H (1984) Processing of regional seismic events using data from small-aperture arrays. Bull Seismol Soc Am 74:2313–2333

Papazachos C, Nolet G (1997) P and S deep velocity structure of the Hellenic area obtained by robust nonlinear inversion of travel times. J Geophys Res 102:8349–8367

Pirli M (2005) A contribution to earthquake location in Greece with the use of seismic arrays. PhD thesis, University of Athens, Athens (in Greek)

Pirli M, Voulgaris N, Alexopoulos J, Makropoulos K (2004a) Installation and preliminary results from a small aperture seismic array in Tripoli, Greece. Bull Geol Soc Greece XXXVI:1499–1508

Pirli M, Voulgaris N, Papadimitriou P, Pavlou K, Makropoulos K (2004b) The Tripoli Seismic Array (TRISAR) contribution to seismic activity monitoring in the Gulf of Corinth and Attica area, Greece, XXIX General Assembly

of the European Seismological Commission, Potsdam 13–17 September 2004, SCB-1, p 9

Pirlis E (2006) Evaluation of the Automatic Data Processing Algorithm and Investigation of Calibration Possibilities for the Tripoli Seismic Array. M.Sc. Thesis, University of Athens, Athens March 2006, p 197 (in Greek)

Rodi W (2006) Grid-search event location with non-Gaussian error models. Phys Earth Planet Inter 158:55–66

Schaff DP, Richards PG (2004) *Lg*-wave cross-correlation and double-difference location: application to the 1999 Xiuyan, China, sequence. Bull Seismol Soc Am 94:867–879

Schweitzer J (2001a) HYPOSAT – an enhanced routine to locate seismic events. PAGEOPH 158:277–289

Schweitzer J (2001b) Slowness corrections – one way to improve IDC products. PAGEOPH 158:375–396

Schweitzer J (2006) How can the ISC location procedures be improved? Phys Earth Planet Inter 158:19–26

Schweitzer J, Fyen J, Mykkeltveit S, Kværna T (2002) Chapter 9: Seismic Arrays. In: Bormann P (ed) IASPEI New Manual of Seismological Observatory Practise (p 52). GeoForschungs-Zentrum, Potsdam

Shearer P (1997) Improving local earthquake locations using the L1 norm and waveform cross-correlation: application to the Whittier Narrows, California, aftershock sequence. J Geophys Res 102:8269–8283

Spakman W (1991) Delay-time tomography of the upper mantle below Europe. Geophys J Int 107:309–332

Sweeney JJ, Walter WR (1998) Preliminary definition of geophysical regions for the Middle East and North Africa, Lawrence Livermore National Laboratory, UCRL-ID-132899, p 40

Wessel P, Smith WHF (1991) Free software helps map and display data. EOS Trans Am Geophys Union 72:441, 445–446

Wessel P, Smith WHF (1998) New, improved version of Generic Mapping Tools released. EOS Trans Am Geophys Union 79:579